Bioinorganic Chemistry

DOI: 10.1002/ange.201407603

X-Ray Emission Spectroscopy: A Spectroscopic Measure for the Determination of NO Oxidation States in Fe–NO Complexes**

Tsai-Te Lu, Tsu-Chien Weng,* and Wen-Feng Liaw**

Abstract: *Extensive study of the electronic structure of Fe-NO complexes using a variety of spectroscopic methods was attempted to understand how iron controls the binding and release of nitric oxide. The comparable energy levels of NO π* orbitals and Fe 3d orbitals complicate the bonding interaction within Fe–NO complexes and puzzle the quantitative assignment of NO oxidation state. Enemark–Feltham notation, $\{Fe(NO)_x\}^n$, was devised to circumvent this puzzle. This 40-year puzzle is revisited using valence-to-core X-ray emission spectroscopy (V2C XES) in combination with computational study. DFT calculation establishes a linear relationship between $\Delta E_{\sigma 2s^*\text{-}\sigma 2p}$ of NO and its oxidation state. V2C Fe XES study of Fe–NO complexes reveals the $\Delta E_{\sigma 2s^*\text{-}\sigma 2p}$ of NO derived from NO $\sigma_{2s}^*/\sigma_{2p} \rightarrow Fe_{1s}$ transitions and determines NO oxidation state in Fe–NO complexes. Quantitative assignment of NO oxidation state will correlate the feasible redox process of nitric oxide and Fe-nitrosylation biology.*

After being discovered as the endothelium-derived relaxing factor (EDRF) and named as molecule of the year in 1992, nitric oxide was reported to trigger versatile signal transduction pathways through Fe-nitrosylation, S-nitrosation of thiol-containing proteins, Tyr-nitration, and N-nitrosation.[1] Among these signal transduction pathways, Fe-nitrosylation features a diverse set of physiological processes and various reaction mechanisms ascribed to alternative Fe active-site structure and feasible redox propensity of nitric oxide. Interplay between the NO and Fe center in different proteins modulates vascular relaxation, transcriptional activation, enzymatic function in Kreb's cycle, and iron homeostasis.[1d,2] Formation of mononitrosyl iron complex (MNIC) through rapid binding of nitric oxide toward the regulatory ferrous heme group of soluble guanylate cyclase (sGC) accelerates the formation of cGMP and activates the vascular relaxation of blood vessels.[1d] Investigation of the biological function of Fe-nitrosylation led to the discovery of dinitrosyl iron complexes (DNICs) during nitrosylation of [Fe-S] proteins, chelatable iron pool (CIP), and ferritin.[2b,3] As a result of nitrosylation, DNICs are one of the major forms for storage of nitric oxide and transnitrosation. Endogenous formation of DNICs derived from nitrosylation of CIP triggers the subsequent transnitrosation to afford cellular S-nitrosothiol.[3a] Induction of NO-dependent upregulation of celluar heat shock protein 70 and in vivo protein S-nitrosylation by treatment of exogenous DNICs was also reported.[4]

Extensive study of the electronic structure of nitrosyl iron complexes using a variety of spectroscopic methods was attempted to understand how the metal iron utilizes its intrinsic reactivity and redox propensity for the stabilization of nitric oxide in the form of Fe–NO complexes.[5] These Fe–NO complexes, in the meantime, are ready to release nitric oxide after accomplishment of NO-related signaling process or encountering with the NO-responsive target. The comparable energy levels of NO π* orbitals and Fe 3d orbitals, however, complicate the Fe–NO bonding interaction and puzzle the quantitative assignment of the oxidation state of Fe-bound nitric oxide as NO^+, NO radical, or NO^-. Invention of Enemark–Feltham notation, $\{Fe(NO)_x\}^n$, circumvents the assignment of NO oxidation state in Fe–NO complexes using n to denote the summation of electrons in Fe 3d orbitals and NO π* orbitals.[6] Herein, this 40-year puzzle is revisited and within reach with the development of valence-to-core X-ray emission spectroscopy (V2C XES) as well as advances in theoretical calculations.

V2C XES was demonstrated as a sensitive probe for the identification of metal-bound ligand(s) and the quantification of small-molecule bond activation.[7] XES displays the dipole-allowed transitions from metal p orbitals to metal 1s orbital after ionization of a metal 1s electron. The XES valence-to-core region, in particular, reveals the ligand np/ns→metal 1s transitions, which are enhanced by a circa 5% contribution of Fe 4p orbitals into the valence orbitals. Upon binding of diatomic molecules toward transition metals (that is, N_2, NO, CO, and CN^-), the delocalization of σ_{2s}* and σ_{2p} orbitals of diatomic molecules into metal 4p orbitals results in the dominant contribution of the σ_{2s}* and σ_{2p} orbitals to the V2C feature.[5g,7c,8] DeBeer and co-workers pioneered in the utilization of this V2C feature for quantifying small-molecule activation and determining the oxidation state of N_2 in iron–dinitrogen complexes.[7c] With regard to this benchmark work, V2C XES in combination with DFT calculation opened a parallel avenue to the determination of the oxidation state

[*] Prof. T.-T. Lu
Department of Chemistry, Chung Yuan Christian University
No. 200, Chung Pei Rd. Chungli, 32023 (Taiwan)
E-mail: TTLu@cycu.edu.tw
Dr. T.-C. Weng
SLAC National Accelerator Laboratory
2575 Sand Hill Rd. Menlo Park, CA 94025 (USA)
E-mail: tsuchien@slac.stanford.edu
Prof. W.-F. Liaw
Department of Chemistry, National Tsing Hua University
No. 101, Section 2, Kuang-Fu Rd. Hsinchu, 30013 (Taiwan)
E-mail: wfliaw@mx.nthu.edu.tw

[**] We gratefully acknowledge the support from staff at ID26 of ESRF. W.-F.L. and T.-T.L. acknowledge financial support from the Ministry of Science and Technology (Taiwan). We also thank Dr. Wei-Ming Ching for helpful discussion.

Supporting information for this article is available on the WWW under http://dx.doi.org/10.1002/anie.201407603.

of NO in Fe–NO complexes. In this study, we demonstrate a case study of mononitrosyl and dinitrosyl iron complexes. V2C XES reveals the transitions from the σ_{2s}* and σ_{2p} orbitals of nitric oxide to Fe 1s orbital and directly probes the energy difference between these two orbitals. This energy difference further quantifies the oxidation state of NO in Fe–NO complexes using the linear relationship between $\Delta E_{\sigma 2s^*\text{-}\sigma 2p}$ of NO and its oxidation state derived from DFT calculation.

In an attempt to test the visualization of the transitions from σ_{2s}* and σ_{2p} orbitals of iron-bound nitric oxide using V2C XES, mononitrosyl iron complex (MNIC) $[Fe(SPh)_3(NO)]^-$ (**1**) ($S = 3/2$) and dinitrosyl iron complexes (DNICs) $[Fe(SPh)_2(NO)_2]^-$ (**2**) and $[Fe(OPh)_2(NO)_2]^-$ (**3**) ($S = 1/2$) embedded in a pseudo-tetrahedral geometry were investigated.[5d,9] Complex $[Fe^{II}(SPh)_4]^{2-}$ containing similar supporting ligands and geometry was used as a reference complex to contrast the contribution of nitric oxide (Figure 1 A).[10] As

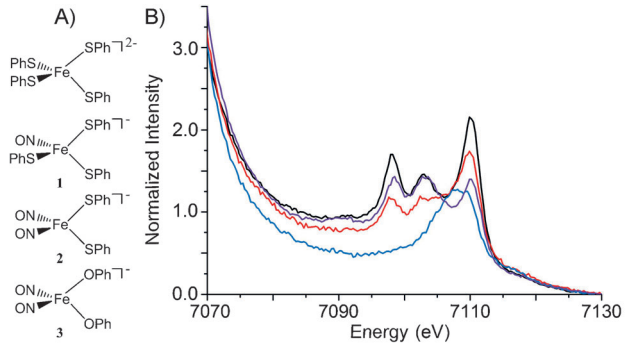

Figure 1. A) Reference complex $[Fe^{II}(SPh)_4]^{2-}$ and nitrosyl iron complexes **1**, **2**, and **3** used in this study. B) Comparison of the normalized Fe K-valence XES spectra of complexes $[Fe^{II}(SPh)_4]^{2-}$ (blue), MNIC **1** (red), DNIC **2** (black), and DNIC **3** (purple).

shown in Figure 1 B, a broad transition peak at 7107.5 eV is observed in the normalized Fe K-valence spectrum of complex $[Fe^{II}(SPh)_4]^{2-}$, as opposed to three distinctive V2C transition peaks at about 7098 eV, 7103 eV, and 7110 eV exhibited by nitrosyl iron complexes **1**, **2**, and **3**. Theoretical calculation was further pursued to verify the nature of these spectral transitions. The deconvolution of the V2C feature of complex $[Fe(SPh)_4]^{2-}$ and the DFT calculated V2C XES spectrum are shown in the Supporting Information, Figure S1, where the corresponding molecular orbitals are depicted in the inset. Based on the DFT calculation, the π-bonding interaction between Fe 3d and S 3p orbitals dominates the V2C feature, while the minor contribution of S 3s orbitals to the V2C feature explains the transition observed at lower energy (ca. 7100 eV).

The experimental V2C XES spectrum and spectral deconvolution of MNIC **1** are presented in Figure 2 A (upper). In comparison with complex $[Fe^{II}(SPh)_4]^{2-}$, the V2C transition peak of MNIC **1** at 7109.1 eV shifts from 7107.5 eV upon replacement of the phenylthiolate ligand by nitric oxide. As shown in Figure 2 B, DFT-calculated V2C XES spectrum resembles the experimental V2C features and rationalizes this energy shift owing to the contribution of the NO π* orbital. Compared to the nature of the V2C feature of homoleptic complex $[Fe(SPh)_4]^{2-}$, this transition presents the π-bonding interactions between the $[Fe(SPh)_3]$ core and nitric oxide. At the lower-energy region, two distinctive V2C transition peaks at 7097.8 eV and 7103.2 eV derived from the incorporation of nitric oxide are observed. DFT calculation provides a computational validation for the dominant contribution from NO σ_{2s}* and σ_{2p} orbitals, respectively, to these XES V2C features together with a circa 5% contribution from Fe p orbitals. Figure 2 A (middle and bottom) depicts the experimental V2C XES spectra of DNICs **2** and **3** together with the representative fit to the data. A similar DFT calculation and analysis was applied to assign the nature of the V2C features observed in DNICs **2** and **3** (Figure 2 B). The molecular orbitals derived from the π-bonding interactions between the $[Fe(XPh)_2]$ core (X = O or S) and NO π* orbitals, similarly, dominates the V2C transition at higher energy (ca. 7109.7 eV). The V2C features at about 7097.9 eV and 7103.3 eV, respectively, mainly originate from the NO σ_{2s}* and σ_{2p} orbitals.

As shown in Table 1, nitrosyl iron complexes **1**, **2**, and **3** show a different V2C transition energy. The dominant contribution of NO σ_{2s}* and σ_{2p} orbitals into the two V2C features at lower energy demonstrates a possible utilization of V2C XES as a spectroscopic measure to directly probe the energy difference between these two orbitals, while the minimal contribution from Fe p orbitals (ca. 5%) has to be taken into account. To test the application of this energy difference to identify the oxidation state of nitric oxide, DFT calculations of oxygen Kα XES spectra of NO^+, NO radical, and NO^- was pursued to establish the linear relationship between $\Delta E_{\sigma 2s^*\text{-}\sigma 2p}$ of NO and its oxidation state.

Table 1: Experimental V2C transition energy of Fe–NO complexes and calculated V2C oxygen Kα transition energy of nitric oxide.

	NO σ_{2s}* [eV]	NO σ_{2p} [eV]	Fe–XPh π-NO π_{2p}*[a] X = O or S [eV]	Δ*E* of NO σ_{2s}*-σ_{2p} [eV]	Oxidation state of NO
1	7097.8	7103.2	7109.1	5.4	-0.58 ± 0.18[b]
2	7097.7	7103.2	7109.6	5.5	-0.77 ± 0.18[b]
3	7097.9	7103.5	7109.8	5.6	-0.95 ± 0.18[b]
NO^+	499.8	504.4	–	4.6	+1.00
NO	497.8	502.8	–	5.0	0.00
NO^-	496.1	501.8	–	5.7	−1.00

[a] The intensity-weighted average energies are given here. [b] Oxidation state of NO in complexes **1**, **2**, and **3** is obtained using the equation $\Delta E\sigma_{2s^*\text{-}\sigma_{2p}} = -0.550$ (oxidation state of NO) + 5.079. A detail discussion of error analysis is included in the Supporting Information.

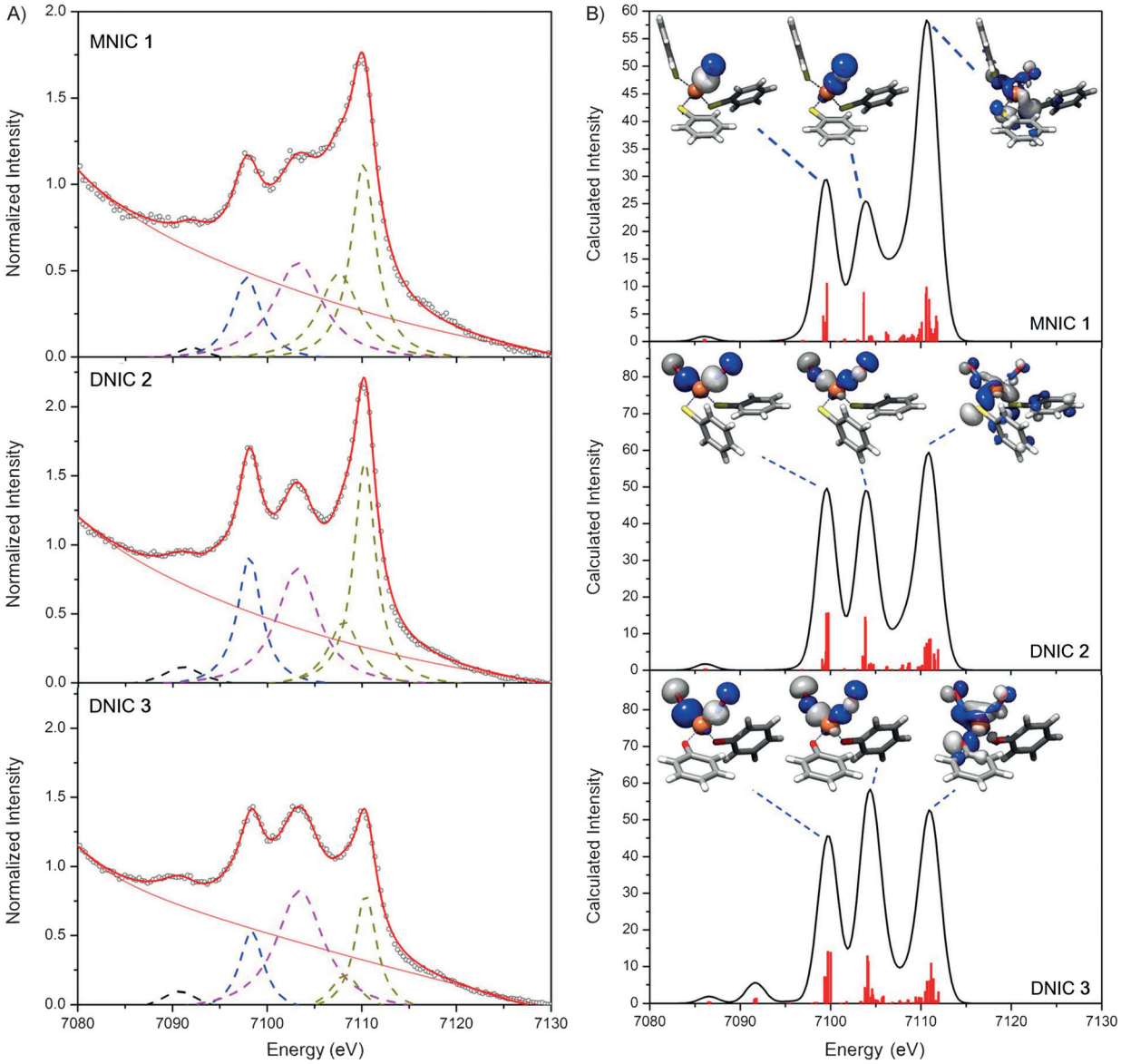

Figure 2. A) Experimental valence-to-core XES spectra (○) of MNIC **1** and DNICs **2**/**3**. Spectral deconvolution of the data is shown as dashed lines. B) DFT calculated valence-to-core XES spectra of MNIC **1** and DNICs **2**/**3**, and the corresponding molecular orbitals for each of the transitions. Calculated peaks are displayed as vertical lines.

Dipole-allowed transitions from NO σ_{2s}, σ_{2s}*, σ_{2p}, and π_{2p} orbitals to the oxygen 1s orbital comprise the calculated oxygen Kα XES spectrum of NO^+, whereas NO radical and NO^- displays an additional transition from occupied NO π_{2p}* orbital(s) to oxygen 1s orbital (Figure 3 A). The calculated oxygen Kα XES spectra of NO with alternative oxidation states display the energy levels of the occupied molecular orbitals derived from oxygen and nitrogen 2s/2p orbitals (Supporting Information, Figure S2). Of importance, the energy difference of the calculated σ_{2s}* and σ_{2p} orbital of NO radical, 5.0 eV, is identical to that of reported binding energies of NO derived from X-ray photoelectron spectroscopy.[11] This consistency calibrates the DFT calculation and validates the further utilization of the linear relationship between $\Delta E_{\sigma 2s^*\text{-}\sigma 2p}$ of NO and its oxidation state. As shown in Figure 3 B, the correlation between $\Delta E_{\sigma 2s^*\text{-}\sigma 2p}$ of NO and its oxidation state follows the equation: $\Delta E_{\sigma 2s^*\text{-}\sigma 2p} = -0.550\,(\text{oxidation state of NO}) + 5.079$. Negative correlation between $\Delta E_{\sigma 2s^*\text{-}\sigma 2p}$ of NO and its oxidation state suggests that the addition of electrons into NO π* orbitals weakens N–O bonding interaction, raises the σ_{2p} orbital, pulls down the σ_{2s}* orbital, and results in the increase of the energy separation between these two orbitals (Supporting Information, Figures S2 and S3).

The absence of NO π_{2p} orbitals interacting with the Fe p orbitals in nitrosyl iron complexes **1**, **2**, and **3** prevents its perturbation on the estimation of $\Delta E_{\sigma 2s^*\text{-}\sigma 2p}$ of Fe-bound nitric oxide using V2C XES, in contrast to the overlap of $\sigma_{2p} \rightarrow O_{1s}$ transition with $\pi_{2p} \rightarrow O_{1s}$ transition at about 502 eV observed in the calculated oxygen Kα XES spectrum of nitric oxide.

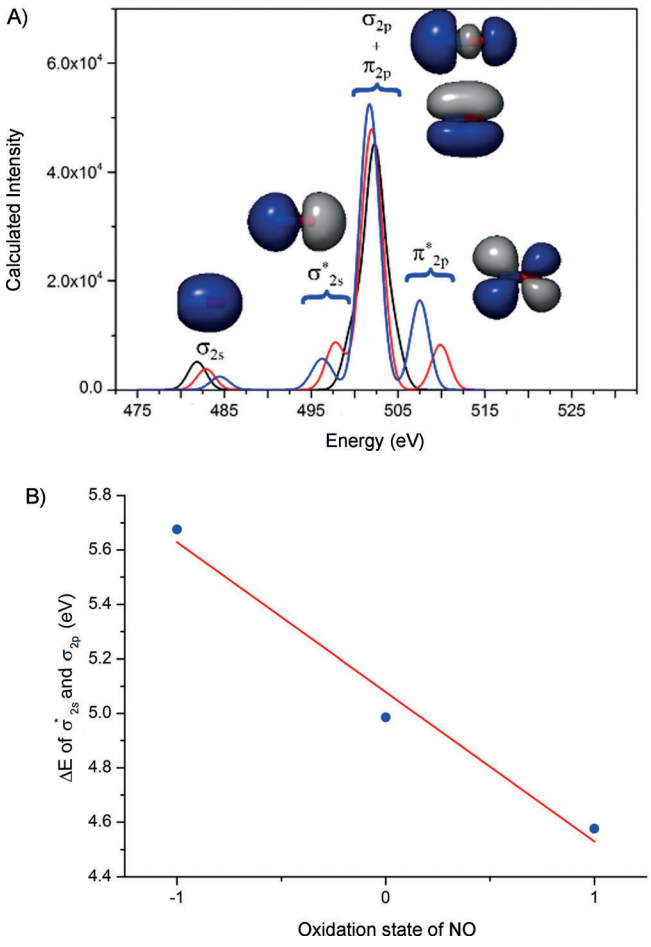

Figure 3. A) DFT calculated oxygen Kα XES spectra of NO^+ (black), NO radical (red), and NO^- (blue). The MO diagrams present the corresponding molecular orbitals for each of the transitions. B) Correlation of the oxidation state of NO and the energy difference between σ_{2s}* and σ_{2p} orbitals of NO. The linear regression line follows the equation $\Delta E\sigma_{2s^*}-\sigma_{2p} = -0.550$ (oxidation state of NO) + 5.079 with a standard error of 0.11.

Energy separation between these two orbitals, in return, discloses the oxidation state of NO in Fe–NO complexes using the equation: $\Delta E_{\sigma 2s^*\text{-}\sigma 2p} = -0.550$ (oxidation state of NO) + 5.079. Based on the $\Delta E_{\sigma 2s^*\text{-}\sigma 2p}$ exhibited by MNIC **1** and DNICs **2**/**3**, the oxidation state of these nitrosyl iron complexes are -0.58 ± 0.18, -0.77 ± 0.18, and -0.95 ± 0.18, respectively (Table 1). Previous spectroscopic study of complexes **1**, **2**, and **3** rationalizes the electronic structure of MNIC **1** as a resonance hybrid of $\{Fe^{II}(NO)\}^7$ and $\{Fe^{III}(NO^-)\}^7$, and that of DNICs **2** and **3** as a resonance hybrid of $\{Fe^{II}(NO)(NO^-)\}^9$ and $\{Fe^{III}(NO^-)_2\}^9$.[5a,c–e,9] Herein, V2C XES quantifies the partial reduction of nitric oxide in the nitrosylation of $[Fe(SPh)_4]^-$ affording MNIC **1** and in the subsequent nitrosylation of MNIC **1** affording DNIC **2** via reductive elimination of phenyldisulfide.[9] Namely, V2C XES quantifies the allocation of the electron, derived from reductive elimination of phenyldisulfide, between Fe and NO upon binding of NO toward $[Fe(SPh)_4]^-$ and MNIC **1**. Moreover, the oxidation state of NO in DNICs **2** and **3** suggests that the replacement of $[SPh]^-$ with $[OPh]^-$ polarizes the Fe–NO bond and enhances the electron transfer from Fe to NO. This finding also suggests that binding of nitric oxide toward non-heme iron, for the sake of the storage and transport of nitric oxide, affords DNICs and stabilizes NO by partial reduction.

In summary, we have demonstrated that valence-to-core X-ray emission spectroscopy reveals the energy separation between σ_{2s}* and σ_{2p} orbitals of Fe-bound nitric oxide and serves as a spectroscopic measure to determine the oxidation state of NO in MNIC and DNIC containing π-donor ligands. With the buildup of V2C Fe Kβ XES as a sensitive probe for oxidation state of NO in Fe–NO complexes, efforts will be made to expand this spectroscopic method to quantify NO oxidation state in a variety of Fe–NO complexes and to brings insights into Fe–NO bonding interaction modulated by its geometric structure and supporting ligands. Furthermore, V2C Fe Kβ XES provides a novel strategy to correlate the interplay between feasible redox process of nitric oxide and Fe-nitrosylation biology, although caution has to be taken on the contribution of supporting ligands to the V2C feature.

Received: July 25, 2014
Published online: September 9, 2014

Keywords: bioinorganic chemistry · iron · nitrosyl complexes · X-ray emission spectroscopy

[1] a) W. P. Arnold, C. K. Mittal, S. Katsuki, F. Murad, *Proc. Natl. Acad. Sci. USA* **1977**, *74*, 3203–3207; b) L. J. Ignarro, R. E. Byrns, G. M. Buga, K. S. Wood, *Circ. Res.* **1987**, *61*, 866–879; c) D. E. Koshland, Jr., *Science* **1992**, *258*, 1861; d) Y. Zhao, P. E. Brandish, D. P. Ballou, M. A. Marletta, *Proc. Natl. Acad. Sci. USA* **1999**, *96*, 14753–14758; e) D. T. Hess, A. Matsumoto, S. O. Kim, H. E. Marshall, J. S. Stamler, *Nat. Rev. Mol. Cell Biol.* **2005**, *6*, 150–166; f) R. Radi, *Proc. Natl. Acad. Sci. USA* **2004**, *101*, 4003–4008; g) N. S. Bryan, T. Rassaf, R. E. Maloney, C. M. Rodriguez, F. Saijo, J. R. Rodriguez, M. Feelisch, *Proc. Natl. Acad. Sci. USA* **2004**, *101*, 4308–4313.

[2] a) B. D'Autreaux, N. P. Tucker, R. Dixon, S. Spiro, *Nature* **2005**, *437*, 769–772; b) M. C. Kennedy, W. E. Antholine, H. Beinert, *J. Biol. Chem.* **1997**, *272*, 20340–20347; c) R. N. Watts, C. Hawkins, P. Ponka, D. R. Richardson, *Proc. Natl. Acad. Sci. USA* **2006**, *103*, 9745–9745.

[3] a) C. A. Bosworth, J. C. Toledo, Jr., J. W. Zmijewski, Q. Li, J. R. Lancaster, Jr., *Proc. Natl. Acad. Sci. USA* **2009**, *106*, 4671–4676; b) M. Lee, P. Arosio, A. Cozzi, N. D. Chasteen, *Biochemistry* **1994**, *33*, 3679–3687.

[4] Y.-J. Chen, W.-C. Ku, L.-T. Feng, M.-L. Tsai, C.-H. Hsieh, W.-H. Hsu, W.-F. Liaw, C.-H. Hung, Y.-J. Chen, *J. Am. Chem. Soc.* **2008**, *130*, 10929–10938.

[5] a) T.-T. Lu, S.-H. Lai, Y.-W. Li, I.-J. Hsu, L.-Y. Jang, J.-F. Lee, I.-C. Chen, W.-F. Liaw, *Inorg. Chem.* **2011**, *50*, 5396–5406; b) J. L. Hess, C. H. Hsieh, S. M. Brothers, M. B. Hall, M. Y. Darensbourg, *J. Am. Chem. Soc.* **2011**, *133*, 20426–20434; c) S. Ye, F. Neese, *J. Am. Chem. Soc.* **2010**, *132*, 3646–3647; d) M.-C. Tsai, F.-T. Tsai, T.-T. Lu, M.-L. Tsai, Y.-C. Wei, I.-J. Hsu, J.-F. Lee, W.-F. Liaw, *Inorg. Chem.* **2009**, *48*, 9579–9591; e) T. C. Harrop, D. Song, S. J. Lippard, *J. Am. Chem. Soc.* **2006**, *128*, 3528–3529; f) L. E. Goodrich, F. Paulat, V. K. Praneeth, N. Lehnert, *Inorg. Chem.* **2010**, *49*, 6293–6316; g) J. E. M. N. Klein, B. Miehlich, M. S. Holzwarth, M. Bauer, M. Milek, M. M. Khusniyarov, G. Knizia, H. J. Werner, B. Plietker, *Angew. Chem. Int. Ed.* **2014**, *53*, 1790–1794; *Angew. Chem.* **2014**, *126*, 1820–1824.

[6] J. H. Enemark, R. D. Feltham, *Coord. Chem. Rev.* **1974**, *13*, 339 – 406.
[7] a) P. Glatzel, U. Bergmann, *Coord. Chem. Rev.* **2005**, *249*, 65 – 95; b) K. M. Lancaster, M. Roemelt, P. Ettenhuber, Y. Hu, M. W. Ribbe, F. Neese, U. Bergmann, S. DeBeer, *Science* **2011**, *334*, 974 – 977; c) C. J. Pollock, K. Grubel, P. L. Holland, S. DeBeer, *J. Am. Chem. Soc.* **2013**, *135*, 11803 – 11808.
[8] a) M. U. Delgado-Jaime, S. DeBeer, M. Bauer, *Chem. Eur. J.* **2013**, *19*, 15888 – 15897; b) C. J. Pollock, S. DeBeer, *J. Am. Chem. Soc.* **2011**, *133*, 5594 – 5601.
[9] T.-T. Lu, S.-J. Chiou, C.-Y. Chen, W.-F. Liaw, *Inorg. Chem.* **2006**, *45*, 8799 – 8806.
[10] K. S. Hagen, J. G. Reynolds, R. H. Holm, *J. Am. Chem. Soc.* **1981**, *103*, 4054 – 4063.
[11] a) K. C. Prince, A. Santoni, A. Morgante, G. Comelli, *Surf. Sci.* **1994**, *317*, 397 – 406; b) K. Siegbahn, *ESCA applied to free molecules*, North-Holland Pub. Co., Amsterdam, **1969**.

